Research Paper

AI-Driven Optimization of Long-Term Potentiation Protocols in an Experimental Model of Alzheimer's Disease

Haleh Fateh [1], Mania Asgharpour [2], Mojtaba Khayat Ajami [1], Seyed Behnamedin Jameie [3], Arya Derakhshesh [4], Mona Farhadi [5], Sobhan Kazemi [6], Hesameddin Allameh [6], Nasrin Hosseini [3*]

[1] *Lifestyle Medicine Research Group, Academic Center for Education, Culture and Research (ACECR), Tehran, Iran*
[2] *Department of Psychology, Karaj Branch, Islamic Azad University, Karaj, Iran*
[3] *Neuroscience Research Center, Iran University of Medical Sciences, Tehran, Iran*
[4] *Student Research Committee, Hamadan University of Medical Sciences, Hamadan, Iran*
[5] *Department of Microbiology, Ka.C., Islamic Azad University, Karaj, Iran*
[6] *School of Medicine, Iran University of Medical Sciences, Tehran, Iran*

Scan to access website

How to cite this paper:
Fateh H, Asgharpour M, Khayat Ajami M, Jameie SB, Derakhshesh A, Farhadi M, et al. AI-Driven Optimization of Long-Term Potentiation Protocols in an Experimental Model of Alzheimer's Disease. Advances in Skin Wound and Tissue Repair. 2025; 22(2):42-47.

10.61882/aswtr.22.2.42

Article info
Received: 04/09/2025
Accepted: 18/09/2025
Published: 27/09/2025

*** Corresponding author:**
Nasrin Hosseini, Neuroscience Research Center, Iran University of Medical Sciences, Tehran, Iran. E-mail: hosseini.n58@gmail.com

ABSTRACT

Background: Alzheimer's disease (AD), is a common neurodegenerative disorder, It is marked by progressive memory loss and cognitive decline. With rapid advances in artificial intelligence (AI), data-driven approaches have become more important in neuroscience research. Animal models are crucial for studying disease mechanisms and testing treatments. However such experiments are often expensive and time-consuming. This study, aimed to refine the experimental protocol for inducing long-term potentiation (LTP) in an AD animal model using AI-driven data mining.

Methods: Electrophysiological data came from male Wistar rats (n = 36) split into control, sham-operated, and AD groups. The AD model was induced by selectively lesioning the Basal Nucleus of Meynert (NBM) with ibotenic acid. Data preprocessing and analysis were done using Python. Feature selection used Mutual Information, Gain Ratio, and Gini Indexcorrelation based filtering involved heatmap visualization. Features with low predictive power or high redundancy were excluded to build a more efficient classification system.

Results: Feature analysis showed Mean Per.PSA.B6–B8 and Mean Per.Slop.B6–B8 were highly predictive pre-tetanic measures (Mean Per.PSA.B3–B4 and Mean Per.Slop.B3–B4) contributed little and were excluded. High-intensity stimulation features (Mean PSA600–1000 and Mean Slop600–1000) provided more value than low – intensity ones (<600mA), so they were kept in the optimized protocol. Correlation analysis confirmed redundancy among low-importance features.

Conclusion: By combining feature importance with correlation-based filtering enabled the identification of key electrophysiological markers were found and redundant variables removed from the LTP protocol. This collection made machine learning models more accurate, stable, and interpretable. It also lowered experimental costs, length, and data requirements. Dimensionality reduction improved computational efficiency and predictive performance, especially with complex models.

Keywords: Alzheimer's Disease; Basal Nucleus of Meynert; Long-term Potentiation (LTP); Artificial Intelligence; Feature Selection; Data Mining; Wistar Rat

Introduction

Alzheimer's disease (AD) is a prevalent and devastating neurodegenerative disorder, it causes progressive deterioration of memory, attention, and learning. Memory dysfunction typically develops insidiously, worsens over time, and ultimately leads to severe dementia. , Neuropathologically, AD is defined by extensive neuronal degeneration .It involves complex biochemical, structural, and behavioral changes, especially in brain regions essential for memory and higher cognitive functions [1].

The basal forebrain cholinergic system is crucial for modulating cortical and subcortical activity. Within this network, the Nucleus Basalis Magnocellularis (NBM; Basal Nucleus of Meynert) sends wide cholinergic projections to the neocortex, olfactory bulb, Broca's area, and basal nuclei. These cholinergic neurons are key

for cognitive processing yet are highly vulnerable to age-related and pathological degeneration [2]. Selective lesioning of the NBM with ibotenic acid serves as a robust experimental model of AD [3]. Clinical and preclinical evidence links greater dementia severity with more extensive cholinergic fiber loss.at the same time ,hallmark features such as β-amyloid plaque closely tie to basal forebrain degeneration [4]. The hippocampus does not receive direct cholinergic input from the basal forebrain, However lesions in the NBM speed hippocampal neurodegeneration through indirect circuitry especially the mossy fiber pathway. Histological evidence supports this, showing decreased choline acetyltransferase activity in the prefrontal cortex and reduced granule cell density in the dentate gyrus after NBM injury [2, 5].

Neuroplasticity, the ability of neurons and synapses to undergo activity-dependent structural and functional modifications, represents the cellular substrate of learning and memory. Among its mechanisms, long-term potentiation (LTP)—a sustained enhancement of synaptic efficacy following high-frequency stimulation—is widely recognized as the electrophysiological correlate of memory encoding. Acetylcholine is a central modulator of cortical and hippocampal plasticity: cholinergic agonists facilitate LTP induction, whereas antagonists impair it [6]. Consequently, the cognitive deficits observed following NBM damage are primarily attributed to cholinergic dysfunction within hippocampal circuitry, with the disruption of acetylcholine-dependent LTP representing a key cellular mechanism underlying AD-related memory impairment [7].

In parallel with these neurobiological discoveries, data-driven approaches and artificial intelligence (AI) have emerged as transformative frameworks for analyzing complex biomedical datasets. Data mining, the principal process of Knowledge Discovery in Databases (KDD), enables the extraction of novel, valid, and interpretable patterns from large volumes of data, thus facilitating predictive modeling and evidence-based decision-making [8]. Within the broad domain of machine learning, artificial neural networks (ANNs)—modeled after the architecture and principles of biological neural systems—have demonstrated consistent success in pattern recognition, classification, and prediction tasks [9]. Their deployment spans numerous biomedical fields, including disease diagnosis, biochemical characterization, medical imaging, and drug discovery [10-12]. Moreover, substantial clinical evidence supports the efficacy of ANN-based models in oncology, cardiology, hematology, infertility, and surgery [13-19], as well as further successful implementations in thyroid disorder classification and cancer detection using decision-tree and support vector machine algorithms [20, 21].

A critical determinant of model performance in machine learning is feature selection, which involves identifying the most discriminative variables (features) while eliminating redundant or non-informative ones. Effective feature selection not only enhances predictive accuracy and model stability but also improves interpretability and reduces computational cost. Established metrics—such as Mutual Information, (a measures of the dependency between variables), Gain Ratio (an adjustment of information gain that accounts for intrinsic information), and the Gini Index (a measure of statistical dispersion for classification) provide systematic strategies for feature ranking and dimensionality reduction, these metrics ensure that only the most relevant features are retained for modeling.

Against this backdrop, the present study was designed to develop and evaluate a machine learning–based framework for classifying electrophysiological patterns of hippocampal activity in a rat model of Alzheimer's disease (AD) induced by selective Nucleus Basalis of Meynert (NBM) lesion. Specifically, we aimed to optimize the long-term potentiation (LTP) recording protocol by identifying the most informative electrophysiological parameters and systematically excluding redundant features. This integrative approach is expected to enhance the accuracy, interpretability, and generalizability of predictive models while reducing the time, cost, and experimental complexity of neurophysiological protocols in Alzheimer's disease research.

Methods

The electrophysiological datasets used in this study were obtained from previously published experiments conducted by our group [22, 23]. Adult male Wistar rats (250–300 g) were randomly assigned to three experimental groups (n = 12 per group): control (C), sham-operated (Sham), and Alzheimer's disease (AD). In the control group, long-term potentiation (LTP) was induced and recorded 21 days after the baseline measurement. In the sham group, normal saline was administered as a vehicle. Recordings were obtained after the same interval. In the AD group, Alzheimer-like pathology was induced by bilateral lesions of the Nucleus Basalis Magnocellularis (NBM) using ibotenic acid. Electrophysiological recordings were performed 21 days post-lesion.

For induction of the AD model, animals were anesthetized with chloral hydrate (450 mg/kg, i.p.) and placed in a stereotaxic frame. Coordinates for the NBM were identified according to the rat brain atlas (AP = –1.2 mm, ML = ±2.3 mm, DV = 7.5 mm). Bilateral injections of ibotenic acid (5 μg/μL, 1 μL per site) were delivered using a Hamilton microsyringe. After recovery, rats were housed individually under standard laboratory conditions.These conditions included a (12-hour light/dark cycle, controlled temperature and humidity, and free access to food and water) [22,23].

Electrophysiological recordings were conducted under urethane anesthesia (1.8 g/kg, i.p.). A bipolar

stainless-steel stimulating electrode (125 μm; Advent, UK) was positioned in the perforant path (AP = –6.9 to –7.2 mm; ML = ±4.0–4.2 mm; DV = 3.2–3.7 mm) .The recording electrode was placed in the granule cell layer of the dentate gyrus (AP = –3.2 to –3.7 mm; ML = ±2.0–2.2 mm; DV = 3.2 mm). Field potentials were amplified, digitized, and analyzed using dedicated electrophysiological software.

Baseline responses were recorded for at least 30 minutes before stimulation. Synaptic efficacy was evaluated by generating input–output (I/O) curves using single-pulse stimulation (100–1000 μA, 0.1 Hz). Five responses were averaged per intensity. Field excitatory postsynaptic potentials (fEPSPs) and population spikes (PS) were quantified. Synaptic strength was expressed as PS amplitude (PSA100–1000) and fEPSP slope (Slope100–1000).

LTP was induced after baseline assessment of 10 I/O responses (100–1000 μA). High-frequency stimulation (HFS) consisted of 10 bursts of 200 pulses delivered at 400 Hz (pulse width: 0.2 ms). Bursts were separated by 10- second intervals. Stimulus intensity was set to 80% of the maximal PS and fEPSP amplitude. Post-tetanic responses were recorded at 40% of maximal intensity. Both fEPSP slope and PS amplitude were measured at 30, 60, and 120 minutes after HFS. Pre-tetanic (PSA B3–B4, Slope B3–B4) and post-tetanic (PSA B6–B8, Slope B6–B8) recordings were included for analysis.

All datasets were processed and analyzed using Python (version 3.9) with the NumPy, SciPy, scikit-learn, and Matplotlib libraries. PSA and slope parameters across stimulation intensities and time points were extracted as input features. Data were saved in CSV format, including feature values and target class labels. Extracted features comprised mean amplitude and slope measures grouped into low-intensity (100–500 μA; Mean PSA100–500, Mean Slope100–500) and high-intensity (600–1000 μA; Mean PSA600–1000, Mean Slope600–1000) categories. Pre-tetanic (Mean Per.PSA.B3–B4, Mean Per.Slope.B3–B4) and post-tetanic (Mean Per.PSA.B6–B8, Mean Per.Slope.B6–B8) values were also included. For classification, control and sham animals were labeled as class 0.AD animals were class 1.

Feature evaluation and ranking were conducted using three established metrics: Mutual Information (MI), Gain Ratio (GR), and Gini Index (GI).These metrics, though initially developed for decision-tree algorithms, are broadly applicable for assessing feature relevance. Decision Tree and Random Forest classifiers were used as interpretable models to validate the rankings. They inherently generate feature-importance scores during training. MI quantified how much each feature reduced uncertainty in predicting the target class; GR corrected for biases linked to features with multiple values. GI measured impurity and reflected a feature's ability to partition data into distinct classes.

To refine model inputs, we used feature selection with ranking and correlation-based filtering. We excluded strongly correlated or weakly informative features were excluded to reduce redundancy and data dimensionality. This approach enhanced model interpretability, reduced computational load, and minimized over fitting. The framework provided a reproducible method to optimize electrophysiological features within the machine learning pipeline, and enabled robust classification of Alzheimer-related patterns.

Results

Table 1 summarizes the results of the feature-importance analysis performed across all extracted electrophysiological parameters. The evaluation used the Gini Index, Gain Ratio, and Mutual Information criteria. This multi-metric approach provides a comprehensive and reliable assessment of each feature's discriminative capacity, . It supports more informed and evidence-based selection for subsequent modeling.

Table 1. Feature importance evaluation based on Gini Index, Gain Ratio, and Mutual Information

Feature	Mutual Information	Gain Ratio	Gini Index
Mean Per.PSA.B6,B7,B8	1.000000	1.000000	1.000000
Mean Per.Slop.B6,B7,B8	0.776686	0.000000	0.000000
Mean Slop.600-1000	0.595083	0.000000	0.182622
Mean PSA600-1000	0.423573	0.000000	0.000000
Mean Per.PSA.B3,B4	0.304121	0.000000	0.000000
Mean PSA100-500	0.232346	0.400781	0.307574
Mean Slop.100-500	0.090279	0.000000	0.000000
Mean Per.Slop.B3,B4	0.000000	0.000000	0.000000

Mean Per.PSA.B6, B7, and B8 achieved the highest across all three metrics (Gini Index, Gain Ratio, and Mutual Information = 1.0), confirming their strong discriminative capacity and relevance for classification. This feature is particularly critical in differentiating AD animals from Control and Sham groups, underscoring its importance for Alzheimer-related analyses.

Similary, while *Mean Per.Slop.B6,B7,B8* obtained a score of zero on the Gini Index and Gain Ratio, it demonstrated a relatively high value (0.776686) in Mutual Information. Although this feature has limited direct classification power, it may nonetheless provide useful complementary information by reducing model uncertainty.

Mean Slop.600–1000 yielded a moderate Gini Index value (0.182622) and a relatively strong Mutual Information score (0.595083), suggesting that although it may not serve as a primary discriminant on its own, it could enhance predictive performance in combination with other features.

By contrast, *Mean PSA600–1000* had a Mutual Information score of 0.423573 despite scoring zero on both Gini Index and Gain Ratio. This indicates that the feature may help reduce uncertainty in classification but contributes minimally to class separation.

Mean PSA100–500 exhibited moderate values for both Gini Index (0.307574) and Gain Ratio (0.400781), suggesting a modest but non-negligible role in classification. However, its Mutual Information score (0.232346) was lower than that of *Mean PSA600–1000*, indicating limited standalone impact.

Mean Per.PSA.B3,B4, and *Mean Slop.100–500* showed very low importance across all metrics (MI = 0.304121 and 0.090279, respectively), highlighting their limited utility in predictive modeling. Similarly, *Mean Per.Slop.B3,B4* scored zero in all three criteria, providing no valuable contribution to classification.

Taken together, the results suggest that pre-tetanic electrophysiological measures (e.g., *PSA B3–B4* and *Slope B3–B4*) contribute minimally to classification accuracy and can be eliminated from the LTP induction protocol without compromising the reliability of outcomes. In contrast, post-tetanic parameters—particularly *Mean Per.PSA.B6,B7,B8*—emerge as the most informative features for distinguishing AD from non-AD groups. These findings highlight opportunities for protocol optimization, reducing the number of redundant recordings while maintaining diagnostic precision. Such streamlining may contribute to significant savings in time, cost, and experimental resources.

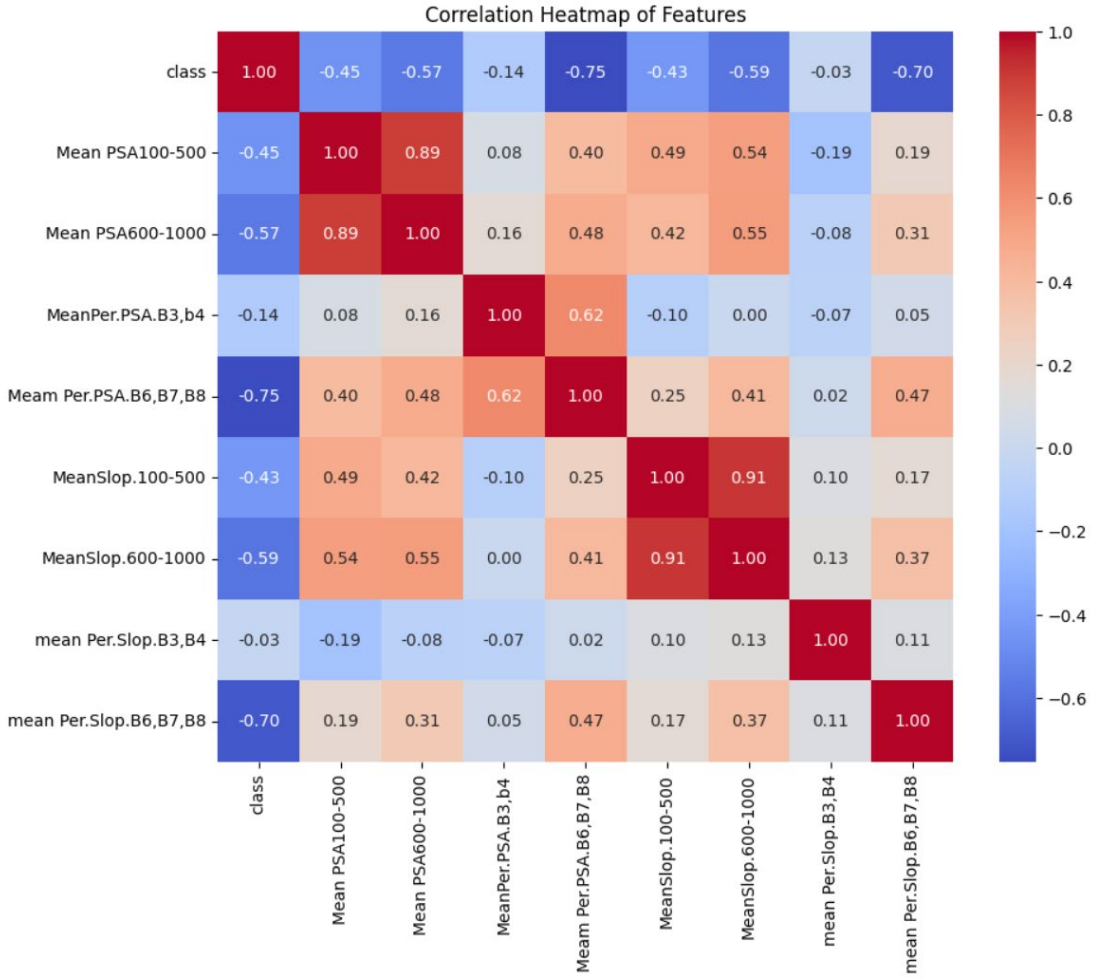

Figure 1. Heatmap visualization of correlations among features

In addition to feature ranking, correlation analysis was performed to examine interrelationships among features and their potential influence on feature selection. A heatmap visualization (Figure 1) was used to depict the correlation matrix, with Pearson's correlation coefficients encoded as color gradients. This graphical representation provided an intuitive means to identify redundant or highly interdependent predictors that could otherwise diminish the discriminative capability of the machine learning models.

For Alzheimer's disease, these analyses are useful for revealing unseen dependencies and highlighting

relationships among electrophysiological measures. By removing redundant or less informative features, we lower dimensionality, making models more efficient and interpretable. Additionally, correlation-based filtering improves model robustness, particularly in complex models, by reducing over fitting and boosting generalization.

As expected, the heatmap showed perfect self-correlation (r = 1.0) along the main diagonal and symmetric pairwise relationships across axes. Although the target variable ("class") was not included as an independent predictor, its associations with other features provided critical insights. The class label demonstrated moderate-to-strong negative correlations with most electrophysiological features (r = –0.03 to –0.75), indicating inverse associations between synaptic measures and Alzheimer-like pathology. Notably, Mean Per.PSA.B6–B8 (r = –0.75) and Mean Per.Slope.B6–B8 (r = –0.70) displayed the strongest negative correlations, underscoring their role as key post-tetanic discriminative features.

Correlation analysis also identified redundancy among predictors. For example, Mean PSA100–500 and Mean PSA600–1000 exhibited a very strong positive correlation (r = 0.89), suggesting overlapping information. Consistent with the feature importance analysis (Table 1), Mean PSA100–500 was excluded due to its lower Mutual Information score. Similarly, Mean Per.PSA.B3–B4 showed a moderate-to-strong correlation (r = 0.62) with Mean Per.PSA.B6–B8 consistently ranked low across all importance criteria; therefore discarded. In addition, a very strong correlation (r = 0.91) between Mean Slope.100–500 and Mean Slope.600–1000 indicated redundancy, leading to the removal of the lower-scoring predictor (Mean Slope.100–500).

Overall, correlation analysis was pivotal in identifying redundant predictors, mitigating multicollinearity, and refining the final feature set. By integrating correlation-based filtering with feature-importance evaluation, the optimized model retained only the most informative electrophysiological parameters while eliminating weak or overlapping variables. This systematic reduction in dimensionality enhanced computational efficiency, improved model robustness, and ultimately increased classification accuracy in distinguishing AD from non-AD groups.

Discussion

This study demonstrates that optimized feature selection is crucial for improving machine learning model performance in Alzheimer's disease research. We systematically appl ied feature-ranking criteria—Mutual Information, Gain Ratio, and the Gini Index—alongside correlation-based filtering. This allowed us to create a structured and reproducible framework for identifying the most discriminative electrophysiological parameters and eliminating redundant or non-informative variables.

A key innovation of this work is combining advanced data-mining strategies with neurophysiological modeling. To our knowledge, this approach has not previously been used for optimizing long-term potentiation (LTP) protocols in Alzheimer's disease models. Previous studies have mostly focused on descriptive electrophysiological outcomes. In contrast, our framework introduces a data-driven, interpretable, and efficient methodology that streamlines experimental design and enhances reproducibility.

By removing one variable from each pair of highly correlated features, we reduced multicollinearity, improved model stability, and simplified the analytical structure. This did not compromise predictive accuracy. The optimized feature set—Mean Per.PSA.B6–B8, Mean Per.Slope.B6–B8, Mean Slope 600–1000, and Mean PSA.600–1000 proved to be strong predictors. These features are both biologically relevant and computationally efficient .Notably, this refined protocol reduces unnecessary electrophysiological recordings. This results in substantial savings in experimental time, cost, and resources.

In summary, this study introduces the first evidence-based, machine learning–guided framework for optimizing LTP induction protocols in an animal model of Alzheimer's disease. This methodology does more than enhance predictive performance. It also improves interpretability, reduces computational complexity, and strengthens model robustness. These findings show the promise of AI-assisted experimental design in neuroscience, especially for accelerating research in neurodegenerative disorders.

Future work should extend this framework to clinical datasets and multimodal biomarkers. By integrating electrophysiological data with neuroimaging, molecular, and behavioral measures, researchers could create comprehensive multimodal predictive models with greater translational impact. Applying this AI-assisted feature selection to human studies may enable personalized diagnostic and therapeutic strategies. This advance would support the move toward precision medicine in Alzheimer's disease and related neurodegenerative conditions.

Acknowledgment

This research was supported by Iran University of Medical Sciences (IUMS) and was conducted under the ethical approval code IR.IUMS.AEC.1404.027. The authors gratefully acknowledge this support.

Practical Implications

This study presents the first evidence-based, machine learning–guided protocol optimization in Alzheimer's research. It links computational intelligence with neurophysiological modeling to speed up discovery.

Funding/Supports

The authors declare that they did not obtain any financial support, grant, or sponsorship from public,

commercial, or nonprofit funding agencies for the conduct of present study.

Author's Contributions

All authors contributed substantially to the conception, design, analysis, and interpretation of the study. Nasrin Hosseini was responsible for the conceptualization of the research, methodology development, and supervision.

Haleh Fateh, Mojtaba Khayat Arjmand, Arya Derakhshesh, Sobhan kazemi, Hesameddin Allameh, and Mania Asgharpour contributed to data collection. Data analysis, and drafting of the manuscript.

Nasrin Hosseini, and Haleh Fateh participated in the interpretation of results.

Mona Farhadi, Seyed Bhnamedin Jameie, nasrin Hosseini, and Haleh Fateh participated in the critical revision of the manuscript, and final approval of the version to be published.

Ethical Considerations

Ethical approval was obtained from the Iran University of Medical Sciences under approval number IR.IUMS.AEC.1404.027

References

1. Zokaei N, Sillence A, Kienast A, Drew D, Plant O, Slavkova E, et al. Different patterns of short-term memory deficit in Alzheimer's disease, Parkinson's disease and subjective cognitive impairment. Cortex. 2020;132:41-50. **doi:** 10.1016/j.cortex.2020.06.016 **pmid:** 32919108
2. Chen XQ, Mobley WC. Exploring the Pathogenesis of Alzheimer Disease in Basal Forebrain Cholinergic Neurons: Converging Insights From Alternative Hypotheses. Front Neurosci. 2019;13:446. **doi:** 10.3389/fnins.2019.00446 **pmid:** 31133787
3. Lecanu L, Papadopoulos V. Modeling Alzheimer's disease with non-transgenic rat models. Alzheimers Res Ther. 2013;5(3):17. **doi:** 10.1186/alzrt171 **pmid:** 23634826
4. Schliebs R. Basal forebrain cholinergic dysfunction in Alzheimer's disease--interrelationship with beta-amyloid, inflammation and neurotrophin signaling. Neurochem Res. 2005;30(6-7):895-908. **doi:** 10.1007/s11064-005-6962-9 **pmid:** 16187224
5. Llorens-Martin M, Blazquez-Llorca L, Benavides-Piccione R, Rabano A, Hernandez F, Avila J, et al. Selective alterations of neurons and circuits related to early memory loss in Alzheimer's disease. Front Neuroanat. 2014;8:38. **doi:** 10.3389/fnana.2014.00038 **pmid:** 24904307
6. Maurer SV, Williams CL. The Cholinergic System Modulates Memory and Hippocampal Plasticity via Its Interactions with Non-Neuronal Cells. Front Immunol. 2017;8:1489. **doi:** 10.3389/fimmu.2017.01489 **pmid:** 29167670
7. Ashkavandi S, Moazedi AA, Semnanian S, Harooni H, Pourmehdi M. Effects of GM1 ganglioside on the recovery of spatial learning after a lesion of the nucleus basalis magnocellularis in an experimental model of Alzheimer's disease in adult male rats. American J Medicine and Medical Sciences. 2015;5(1):42-7.
8. Piatetsky-Shapiro G, Parker G. Data mining, and knowledge discovery: An Introduction. In: Piatetsky-Shapiro G, editor. Journeys to Data Mining2012. p. 173-96.
9. Umek L, Zupan B, Toplak M, Morin A, Chauchat J-H, Makovec G, et al. Subgroup Discovery in Data Sets with Multi–dimensional Responses: A Method and a Case Study in Traumatology. Artificial Intelligence in Medicine. Lecture Notes in Computer Science2009. p. 265-74.
10. Muñoz S. Time-varying network models of neurodegenerative disease spread in biological neural networks. SUNFEST.64.
11. Khan IY, Zope P, Suralkar S. Importance of artificial neural network in medical diagnosis disease like acute nephritis disease and heart disease. International journal of engineering science and innovative technology (IJESIT). 2013;2(2):210-7.
12. Kosik KS. Diseases: Study neuron networks to tackle Alzheimer's. Nature. 2013;503(7474):31-2. **doi:** 10.1038/503031a **pmid:** 24218661
13. Tahamtan RAM, Esmaeili MH, Ghaemian A, Esmaeili J. Application of artificial neural network for assessing coronary artery disease. Journal of Mazandaran University of Medical Sciences. 2012;22(86):8-17.
14. Salehi M, Gohari M, Vahabi N, Zayeri F, Yahyazadeh S, Kafashian M. Comparison of artificial neural network and cox regression models in survival prediction of breast cancer patients. Journal of Ilam University of Medical Sciences. 2013;21(2):120-8.
15. George J, Ahmed A, Patnaik M, Adler Y, Levy Y, Harats D, et al. The prediction of coronary atherosclerosis employing artificial neural networks. Clin Cardiol. 2000;23(6):453-6. **doi:** 10.1002/clc.4960230616 **pmid:** 10875038
16. Kaufmann SJ, Eastaugh JL, Snowden S, Smye SW, Sharma V. The application of neural networks in predicting the outcome of in-vitro fertilization. Hum Reprod. 1997;12(7):1454-7. **doi:** 10.1093/humrep/12.7.1454 **pmid:** 9262277
17. Nilsson J, Ohlsson M, Thulin L, Hoglund P, Nashef SA, Brandt J. Risk factor identification and mortality prediction in cardiac surgery using artificial neural networks. J Thorac Cardiovasc Surg. 2006;132(1):12-9. **doi:** 10.1016/j.jtcvs.2005.12.055 **pmid:** 16798296
18. Kurt I, Ture M, Kurum AT. Comparing performances of logistic regression, classification and regression tree, and neural networks for predicting coronary artery disease. Expert Systems with Applications. 2008;34(1):366-74. **doi:** 10.1016/j.eswa.2006.09.004
19. Biglarian A, Hajizadeh E, Kazemnejad A, Zayeri F. Determining of prognostic factors in gastric cancer patients using artificial neural networks. Asian Pac J Cancer Prev. 2010;11(2):533-6.
20. Aswani Kumar S, Lakshmipathi B, JacqulinMargret J. Diagnosis of Thyroid Disorders using Decision Tree Splitting Rules. International Journal of Computer Applications. 2012;44(8):43-6. **doi:** 10.5120/6287-8474
21. Chang C-Y, Tsai M-F, Chen S-J. Classification of the thyroid nodules using support vector machines. 2008 IEEE International Joint Conference on Neural Networks (IEEE World Congress on Computational Intelligence)2008. p. 3093-8.
22. Hosseini N, Alaei H, Reisi P, Radahmadi M. The effects of NBM- lesion on synaptic plasticity in rats. Brain Res. 2017;1655:122-7. **doi:** 10.1016/j.brainres.2016.11.013 **pmid:** 27867034
23. Hosseini N, Alaei H, Reisi P, Radahmadi M. The effect of treadmill running on memory before and after the NBM-lesion in rats. J Bodyw Mov Ther. 2013;17(4):423-9. **doi:** 10.1016/j.jbmt.2012.12.005 **pmid:** 24138998